



1 **Environmental and vegetation control on the active layer and soil** 2 **temperature in an Arctic tundra ecosystem in Alaska**

3 Kevin J. Gonzalez Martinez^{1,3}, Donatella Zona¹, Trent Biggs², Kristine Bernabe¹, Danielle Sirivat^{1,4},
4 Francia Tenorio^{1,3,4}, Walter Oechel¹

5 ¹Department Biology, San Diego State University, San Diego, CA 92182, USA

6 ²Department Geography, San Diego State University, San Diego, CA 92182, USA

7 ³NOAA EPP/MSI Center for Earth System Sciences and Remote Sensing Technologies II Fellow

8 ⁴Department of Land, Air and Water Resources, University of California at Davis, United States

9 *Correspondence to:* Kevin J. Gonzalez (kevinjgonzalezmartinez@gmail.com) & dzona@sdsu.edu

10 **Abstract.** Permafrost soils contain approximately twice the amount of carbon than the atmosphere, which could be released
11 as global warming continues. Increasing global temperatures have in fact the potential to result in increased permafrost
12 degradation, and carbon loss into the atmosphere. To properly understand the potential release of the carbon stored in
13 permafrost soils, it is critical to understand the environmental and vegetation control on the development of active layer, the
14 upper soil layer that thaw during the growing season in the Arctic. Arctic tundra ecosystems are dominated by mosses, which
15 compose approximately 40% of the vegetation, and have a critical role in regulating the heat condition into the soil. Given
16 their importance, the role that mosses play on permafrost degradation should be investigated in more details. This study
17 measured soil temperature together with thaw depth, a range of environmental variables, and moss thickness, to identify the
18 most important controls on the development of the active layer across 124 plots in continuous permafrost tundra ecosystems.
19 We found that a thicker moss layer insulated the soil and resulted in cooler temperatures deeper in the soil, despite warmer
20 surface temperatures. A thicker moss layer was associated with a deeper depth of thaw, likely for the higher growth of mosses
21 in the drier and warmer topographically higher elevation areas. The protective role of mosses was only relevant for the first ~3



22 cm of the green moss layer, suggesting that the living moss layer was more important in regulating soil temperature, possibly
23 through a higher ability to retain water. Soil moisture was in fact an important control on surface and deeper soil temperatures,
24 with wetter soils been associated with cooler surface temperatures because of the higher evaporative cooling, and warmer
25 deeper temperatures likely because of the larger heat conduction to deeper soils. Overall, this study highlights the importance
26 of a green living moss layer on soil temperature and thaw depth. Mosses are among the most vulnerable vegetation to
27 hydrological changes, given their lack of a rooting system, and their sensitivity to climate change should be considered when
28 predicting the response of permafrost thaw to climate change.

29

30 **Short summary**

31 Permafrost soils contain twice the amount of carbon than the atmosphere, and its release could majorly affect global
32 temperatures. This study found that a thicker moss layer resulted in cooler temperatures deeper in the soil, despite warmer
33 surface temperatures. The top green living moss layer was the most important in regulating the soil temperatures and should
34 be considered when predicting the response of permafrost thaw to climate change.

35

36 **1 Introduction**

37 Northern high-latitude ecosystems are characterized by the presence of permafrost, a soil layer that remains frozen for at least
38 two consecutive years (Permafrost Subcommittee 1988). The active layer (also known as the thaw depth) is the layer of soil
39 of variable depth found directly above the permafrost which only thaws during the summer (Permafrost Subcommittee 1988).
40 The depth of this active layer depends on a combination of factors, including abiotic factors such as air temperatures, solar
41 radiation, and soil moisture, which may increase subsurface heat and associated belowground thermal difference (Dafflon et
42 al. 2017; Fisher et al. 2016; Permafrost Subcommittee 1988; Schuur et al. 2015; Williams et al. 2020). Vegetation also has a
43 role in the development of the active layer by potentially decreasing heat transfer below the surface by serving as a layer of
44 insulation when dry or increasing heat transfer when wet (Beringer et al. 2005; Blok et al. 2010; Blok et al. 2011; Hayashi et
45 al. 2007; Hrbáček et al. 2020; Park et al. 2018; Porada et al. 2016). Globally, permafrost and the active layer currently store



46 an estimated 15 gigatons of carbon (Koven et al. 2011; Schurr 2019). The increasing severity of climate change currently
47 threatens the stability of this sequestered carbon (Miner et al. 2022; Schaphoff et al. 2013; Schuur et al. 2008). The release of
48 the vast carbon stored in these high-latitude soils can potentially affect the climate at the global scale through positive feedback
49 loops in which increased atmospheric carbon may further greenhouse emissions and permafrost degradation (Davidson and
50 Janssens 2006; Schuur et al. 2008). These positive feedback loops further contribute to the rapid change in climate in the
51 northern high-latitude ecosystems known as “Arctic amplification” (Dai et al. 2019).

52 Given the large carbon store of permafrost soils (Hugelius et al. 2014), it is critical to improve understanding of the
53 environmental and vegetation controls on active layer development. Mosses comprise approximately 40% of the Arctic
54 sedge tundra and exist in “mats” alongside other forms of vegetation directly above permafrost soils and their associated ice
55 wedges (Euskirchen et al. 2009). Mosses play a significant role in regulating thaw depths by reducing the heat penetration
56 belowground when dry or increasing it when wet (Beringer et al. 2005; Blok et al. 2010; Blok et al. 2011; Hayashi et al. 2007;
57 Hrbáček et al. 2020; Park et al. 2018). Mosses retain a unique adaptation to desiccation that allows them to desiccate while
58 remaining alive and to create a layer of tissue, which thermally insulates soils (Blok et al. 2011; Park et al. 2018). The dried
59 mats have an insulation effect with increased moss community coverage and layer thickness associated with lower soil
60 temperatures in deeper soil layers and a shallower active layer depth (Blok et al. 2011; Park et al. 2018; van der Wal et al.
61 2001). A wetter moss layer should result in increased heat conduction in the soil and a deeper active layer depth (Hayashi et
62 al. 2007; Hrbáček et al. 2020; Park et al. 2018).

63 The overall control that mosses and other environmental drivers have on permafrost degradation is still not fully understood
64 (Fisher et al. 2018; Luo et al. 2016). The Arctic is experiencing warmer temperatures and increased precipitation between
65 August to October (Boisvert and Strove 2015, Fujinami et al. 2016). The resulting increase in moisture availability can increase
66 thermal conduction in deeper soil layers in turn supporting thawing of the soil (Beringer et al. 2005; Blok et al. 2011; Hayashi
67 et al. 2007; Hrbáček et al. 2020; Park et al. 2018). This increase in thermal conduction may lead to increased permafrost soil
68 thawing which in turn would lead to increased releases of greenhouse gas emissions (Miner et al. 2021; Schaefer et al. 2014;



69 van Huissteden and Dolman 2012). Therefore, an increased depth of thaw can create a positive feedback loop which can further
70 exacerbate the effects of climate change in the Arctic.

71 To further our understanding of the controls on the development of the active layer, a range of environmental drivers and
72 vegetation characteristics should be investigated, including soil moisture, solar radiation, and air and soil temperatures together
73 with the thickness of the moss mat across the fine scale, micro topographically variable polygonal tundra ecosystems. The goal
74 of this research is to identify the biotic and abiotic controls regulating soil temperature and the thawing of the active layer
75 across a range of microtopographic areas in a wet sedge arctic tundra ecosystem in Alaska. We expect thicker mosses to be
76 associated with shallower depth of thaw and decreased belowground temperatures. We anticipate moss patches with increased
77 soil water content to be associated with deeper depth of thaw as well as increased belowground temperatures given an increase
78 in heat conduction with higher soil moisture.

79 **2 Methods**

80 **2.1 Study Sites**

81 The sites of this research are near Utqiagvik, Alaska (formerly known as Barrow), which is the largest town in the Alaskan
82 North Slope Borough. Our team has been maintaining several micrometeorological and eddy covariance towers in Utqiagvik
83 over the last decades (Zona et al., 2016). This research was conducted near two of these eddy covariance towers, which were
84 in operation from 2005-2009 (Fig. 1b, the US-Ben (North), and US-Bec (Central) sites, established during the Biocomplexity
85 Experiment, see Zona et al., 2009; Zona et al., 2012). Environmental drivers (such as air temperature and photosynthetic active
86 radiation (PAR)) measured from another tower still operational since 2005 (US-Bes), in close proximity to the US-Ben and
87 US-Bes sites, were also included in this study. The locations of the US-Bes, US-Bec, and US-Ben are: 71.2809N, -156.5965W;
88 71.28316N, -156.60342W; and 71.28628N, -156.60424W respectively (Zona et al., 2009). These sites are located in a drain
89 lake basin ecosystem with vegetation classified as wet sedges tundra dominated by mosses, lichens, and graminoids with
90 patches of water and partially to fully submerged patches of vegetation (Davidson et al., 2016). Given the proximity of these
91 sites (US-Ben and US-Bec being within 662-meters and 356-meters of US-Bes respectively), we assume that the air



92 temperature and PAR collected in US-Bes were representative of the US-Ben and US-Bec sites. Access to US-Bes, US-Bec,
93 and US-Ben sites was facilitated by the establishment of boardwalks during the Biocomplexity experiment in summer 2005
94 (Zona et al., 2009). These boardwalks allowed sampling across the sites while limiting disturbance. Data was collected every
95 two meters in both US-Ben and US-Bec across 124-meters transects that parallel historical water table data collection (Zona
96 et al., 2012), for a total of 62 plots in US-Ben and 62 in US-Bec.



97

98 **Figure 1: Study site: (a) Map of Alaska showing the general location of Utqiagvik accessed via ©Google Earth Pro**
99 **Copernicus/Landsat satellite imagery (2023). (b) A high-resolution orthorectified camera imagery mosaic acquired by the National**



100 **Ecological Observatory Network (NEON) Airborne Observation Platform (AOP) highlighting the US-Ben and US-Bec transects**
101 **(with the transect lengths highlighted in blue) and the US-Bes tower site. (c) The CR3000 datalogger with 21 thermocouples for**
102 **belowground and air temperature recordings every centimetre. (d) A cross section of the moss layer showing the total (lowest brown**
103 **point to surface) moss layer thickness and green (living) moss layer thickness. (e) A photograph of the research site, showing the**
104 **boardwalk used for sampling.**

105

106 **2.2 Vegetation and environmental controls**

107 The data collection was performed at 2-meter intervals along two 124-meter transects at US-Bec and US-Ben (Fig. 1b). In
108 each of these plots we recorded the thickness of the total moss layer and the thickness of the green living moss layer. A previous
109 in-depth vegetation analysis from our team showed that the general region where this data was collected was composed
110 primarily of graminoids as the dominant vascular plant group, and by mosses such as *Sphagnum sp.* and *Drepanocladus sp.*
111 (Davidson et al., 2016). We also collected data on the dominant moss genus at every point and found *Sphagnum sp.* and
112 *Drepanocladus sp.* to be the dominant genera at our sites with most of the plots being *Sphagnum sp.* (N = 55) or some
113 combination of predominantly *Sphagnum sp.* and *Drepanocladus sp.* (N = 46) and a limited number of plots with only
114 *Drepanocladus sp.* (N = 21). The moss layer thickness and genus identification were recorded in sections of approximately
115 25-square cm (5 cm x 5 cm) in each of the 2-meter plots only once (i.e., the first week of July in 2021 for all plots and a subset
116 of these plots on the first week of July in 2022) during the peak season (i.e., the first week of July to the second week of August
117 2021) to reduce the disturbance to the moss layer. These sections were carefully removed using a serrated knife trying to limit
118 damage to surrounding vegetation. Afterwards, the thickness of the moss mat was measured with a ruler (Fig. 1d), and the
119 samples were reinserted into the sampling locations.

120 In each of the plots for each of the sites (N=62 US-Ben, and N=62 for US-Bec) we also recorded moss and soil temperature
121 every cm from 1 cm below the surface until 20 cm below ground on a weekly basis using type T thermocouples connected to
122 a CR3000 datalogger (Campbell Scientific, Logan, UT, USA). These temperature profiles allowed us to determine how the
123 presence and thickness of the moss layer affected the thermal difference across the moss and soil layers. These 21



124 thermocouples were attached to a fiberglass probe, which facilitated insertion in the moss layer and soil. Each point was
125 measured for approximately 3 minutes as the temperature readings stabilized within the first couple of minutes. We also
126 collected soil water content (percent water) weekly in the first 5-cm of the moss or soil layer using a FieldScout TDR300
127 (Spectrum Technologies, Aurora, IL, USA) and 5-cm rods (Beringer et al., 2005; Hayashi et al., 2007; Hrbáček et al., 2020).
128 The FieldScout was calibrated using local water samples to account for nutrients which may influence conductivity. Thaw
129 depth and water table levels were also collected weekly in each of the sampling plots using a metal and wooden probe
130 respectively with markings indicating intervals of 1-cm depths. Water table measurements were collected inside PVC pipes
131 (with holes every 1 cm) previously installed along the transects (Zona et al., 2009; Zona et al., 2012) in each of the sampling
132 locations. This data collection was repeated for a second field season in a subset of the plots (N = 20 in Summer 2022 vs. N =
133 124 in Summer 2021) to reduce disturbance to the sites; samples collected in these different years were compared, showing
134 good agreement between the measured moss thickness in the 2021 and 2022 field seasons ($R^2 = 91.82\%$, $p\text{-value} < 0.001$, 2022
135 Moss Thickness (cm) = $1.01967 * 2021 \text{ Moss Thickness (cm)} + 0.228272$).

136 Environmental variables collected by the eddy covariance US-Bes tower, included PAR, air temperature, local surface and
137 subsurface soil temperature, relative humidity, wind speed, and net radiation. Elevation above sea level was collected in each
138 of the sampling plots at US-Ben and US-Bec with a dGPS as reported in Zona et al. (2012). These measurements described
139 the microtopography of each of the sampling plots and allowed us to test the role on microtopography on the environmental
140 conditions, vegetation, and active layer development.

141

142 **3 Statistical Analysis**

143 All statistical analyses were conducted using R version 4.2.0 (R Core Team, 2022); the caret, leaps, and MASS packages
144 (Kuhn, 2022; Lumley and Miller, 2022; Posit Team, 2022; R Core Team, 2022; Venables and Ripley, 2002), and stepwise
145 multiple regressions and univariate regressions (both linear and nonlinear) were used to test for and model the relationships
146 between the deepest (minimum given the negative sign) thaw depth (D_{thaw}) or the temperature difference between 1 and 15 cm



147 belowground (dT_{1-15}) and environmental predictors, and to evaluate the collinearity in predictors. For the stepwise multiple
148 regressions, we tested the correlations between predictor variables, given that covarying variables can create issue when
149 included together in the same model; variables that met cutoff points ($-0.65 \geq r \geq 0.65$ and $p\text{-value} < 0.05$) were not included
150 together in the stepwise multiple regression models. Data from both 2021 and 2022 were aggregated by both site and distance
151 along each transect. The predictor variables included median, maximum, and minimum values of water table level, soil water
152 content, temperature at 15 cm belowground, 10 cm belowground, 5 cm belowground, 1 cm belowground, 5 cm aboveground,
153 green moss layer thickness, total moss layer thickness, and PAR. Deviation from the mean elevation (dz) was calculated as a
154 simple difference between each elevation point and the mean elevation. dT_{1-15} was calculated as the difference in temperatures
155 recorded at 1 cm belowground and 15 cm belowground; -15 cm was selected as it was the thaw depth most consistently
156 represented at most of the sites during the entire collection period. We used the median dT_{1-15} for each plot along each transect
157 for both 2021 and 2022, given that only one elevation value was recorded for each plot. We tested the influence of moss genus
158 on the statistical analysis but did not find it significant, so we did not include it in the results.

159 dT_{1-15} was modelled as a function of the median air temperature, dz , the soil water content, and both the midsummer green
160 and total moss layer thicknesses. We tested the relationship between D_{thaw} as a function of dz , median water table level, median
161 soil water content, maximum soil temperatures, median local air temperatures, 2021 midsummer green and total moss layer
162 thicknesses, median PAR, and dT_{1-15} . dT_{1-15} was regressed against the median water table level, median soil water content,
163 D_{thaw} , median local air temperatures, green and total moss layer thicknesses, median PAR, and dz . We tested the collinearity
164 of predictor variables; covarying variables ($-0.65 \geq r \geq 0.65$ and $p\text{-value} < 0.05$) were not included together in the stepwise
165 regression models, and each variable was also tested separately in a univariate model to rank their relative importance as
166 explanatory variable.

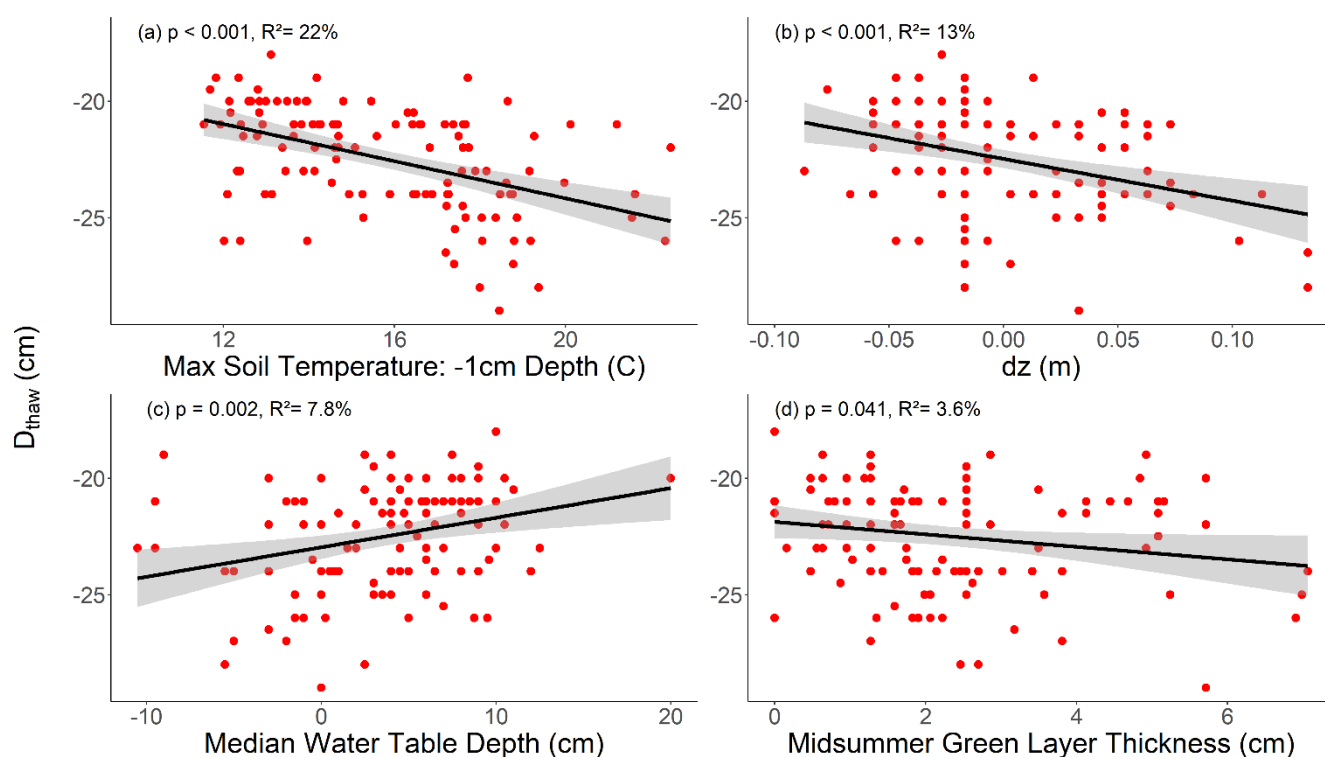
167 To evaluate the environmental controls on either thaw depth, and soil temperature (at -1 cm and -15 cm depth), we tested a
168 variety of non-linear regressions, including different order polynomial and logarithmic regressions, given that ecological
169 processes can have complex relationships (Zona et al., 2023). However, when evaluating these models, we did not find an
170 ecological explanation for the statistical models with the highest explanatory power which were at the time third order



171 polynomial models. Therefore, we applied piecewise regressions to test the occurrence of a breakpoint in the linear regressions,
172 using the segmented package in R (Muggeo, 2003; 2008). When the occurrence of a breakpoint was significant, we included
173 separate linear regressions for the two datasets separated by the breakpoint.

174

175 4 Results



176

177 **Figure 2: Relationship between the deepest thaw depth (D_{thaw}) and the indicated variables for the entire study period (summer 2021**
178 **and 2022) and for both study sites combined, demonstrating a) a negative relationship between the maximum soil temperature at -**
179 **1 cm depths and deepest thaw depth, b) a negative relationship between the deviation from the mean elevation (dz) and the deepest**
180 **thaw depth, c) a positive relationship between water table level and the deepest thaw depth, and d) a negative relationship between**
181 **green moss layer thickness during the middle of the 2021 summer and the deepest thaw depth.**



182 Several environmental variables were strongly correlated (Table S1). The strongly correlated variables ($-0.65 \geq r \geq 0.65$ and
183 p -value < 0.05) were not included together in the regression models of D_{thaw} , dT_{1-15} , and soil temperature at -1 and -15 cm. See
184 Table S1 for details on the correlation coefficients and p -values among those variables.

185 The maximum temperature for each measurement point aggregated across both years at -1 cm belowground had the highest
186 explanatory power in the stepwise model of the deepest thaw depth for each measurement point aggregated across both years
187 (p -value < 0.001 , $R^2 = 22\%$, Akaike information criterion (AIC) = 500, Table 1). A similar result was obtained from the
188 comparison of univariate regressions, where the maximum soil temperature at -1 cm had the highest explanatory power on the
189 variability of thaw depth. The stepwise model for dT_{1-15} identified the median soil water content, deepest thaw depth, and dz
190 as the only significant variables among the variables tested (i.e., median soil water content, the deepest thaw depth, median air
191 temperature, total moss layer thickness, and the dz , p -value < 0.001 , $R^2 = 45\%$, AIC = 525, Table 2). A complete list of the
192 statistics of the univariate models are included in Tables 3 and 4.

193 **Table 1: Statistics of the stepwise linear regression model of the deepest thaw depth (cm) for summer 2021 and 2022 across all the**
194 **plots, which selected the maximum soil temperature at -1 cm depth as the variable with the highest explanatory power and the only**
195 **significant predictor. Included are the regression coefficient, R^2 , p -value, the Akaike information criterion (AIC).**

Deepest Thaw Depth				
Variable	Coefficient	R^2	p -value	AIC
Maximum Soil Temperature – -1 cm	-0.40	22%	< 0.001	500

196

197 **Table 2: Statistics of the stepwise linear regression model of the temperature difference between the 1 and 15 cm depths (dT_{1-15})**
198 **which selected the following variables as those with the highest explanatory power. Included are the coefficients, R^2 , p -values, and**
199 **the Akaike information criterion (AIC). The overall p -value for the entire model was < 0.001 .**



Temperature Difference				
Variable	Coefficient	R ²	p-value	AIC
Median Soil Water Content	-0.09		0.003	
Deepest Thaw Depth	-0.33	45%	0.001	525
Deviation from the Mean Elevation (dz)	27.94		< 0.001	

200

201 After ranking and comparing all models including the variables listed in Table S1, maximum soil temperatures at -1 cm, dz,
 202 median water table level, and green moss layer thickness explained the largest percentage of variation in the deepest thaw
 203 depth (Fig. 2). Soil temperature alone explained about 22% of the variability in the deepest thaw depth (Table 1). Similarly,
 204 dT₁₋₁₅ was mostly explained by the dz, soil water content, and green and total moss layer thicknesses (Fig. 3). The dz had the
 205 highest explanatory power explaining 34% of the variability in dT₁₋₁₅ (Fig. 3), and the addition of soil water content and the
 206 deeper thaw depth increased the explanatory power to 45% (Table 2).

207

208 **Table 3: Statistics of the univariate simple linear regressions of the deepest thaw depth and the indicated variables including the**
 209 **entire dataset. The variables are ranked based on the simple linear model's R² value. Included are the R², p-value, the Akaike**
 210 **information criterion (AIC), and the breakpoint if statistically significant.**

Deepest Thaw Depth				
Predictor Variable	Breakpoint	R ²	p-value	AIC



Maximum Soil				
Temperature – -1 cm	N/A	Linear: 22%	Linear: < 0.001	Linear: 500
Belowground				
Temperature Difference	N/A	Linear: 19%	Linear: < 0.001	Linear: 504
Median PAR	N/A	Linear: 13%	Linear: <0.001	Linear: 512
Difference from Mean Elevation	N/A	Linear: 13%	Linear: < 0.001	Linear: 513
Median Water Table Level	N/A	Linear: 7.8%	Linear: 0.002	Linear: 519
Maximum Soil				
Temperature – 5 cm	N/A	Linear: 7.1%	Linear: 0.004	Linear: 520
Green Moss				
Layer Thickness	N/A	Linear: 3.6%	Linear: 0.041	Linear: 524

211

212 **Table 4. Statistics of the univariate simple linear and piecewise regressions of the temperature difference (dT_{1-15}) and the indicated**
 213 **variables including the entire dataset. Included are the R^2 , p-value, the Akaike information criterion (AIC), and the breakpoint if**
 214 **statistically significant. The significance in the difference between models is included in the column “ANOVA” only when the p-**
 215 **value was less than 0.05 (e.g., the significance in the difference between the linear (L) and the piecewise (PW) was 0.005 for the**
 216 **median local air temperature). The best models are highlighted in bold.**

Thermal Difference



Variable	Breakpoint	R ²	p-value	AIC	ANOVA
Median PAR	N/A	Linear: 43%	Linear: < 0.001	Linear: 523	
		Linear: 41%	Linear: < 0.001	Linear: 528	
Median Local Air Temperature	x = 12.6	x < 12.6: 12%	x < 12.6: < 0.001	x < 12.6: 539	L-PW: 0.005
		x > 12.6: 50%	x > 12.6: 0.049	x > 12.6: 36.7	
		Linear: 40%	Linear: < 0.001	Linear: 530	
Median Water Table Level	x = -1.1	x < -1.1: 6.3%	x < -1.1: 0.330	x < -1.1: 67.3	L-PW: < 0.001
		x > -1.1: 42%	x > -1.1: < 0.001	x > -1.1: 448	
Difference from Mean Elevation	N/A	Linear: 34%	Linear: < 0.001	Linear: 541	
Minimum (Deepest) Thaw Depth	N/A	Linear: 19%	Linear: < 0.001	Linear: 566	
		Linear: 15%	Linear: < 0.001	Linear: 570	
Median Soil Water Content	x = 74.4	x < 74.4: 0.36%	x < 74.4: 0.725	x < 74.4: 167	L-PW: < 0.001
		x > 74.4: 19%	x > 74.4: < 0.001	x > 74.4: 381	
		Linear: 14%	Linear: < 0.001	Linear: 572	
Green Moss Layer Thickness	x = 3.1	x < 3.1: 21%	x < 3.1: < 0.001	x < 3.1: 439	L-PW: < 0.001

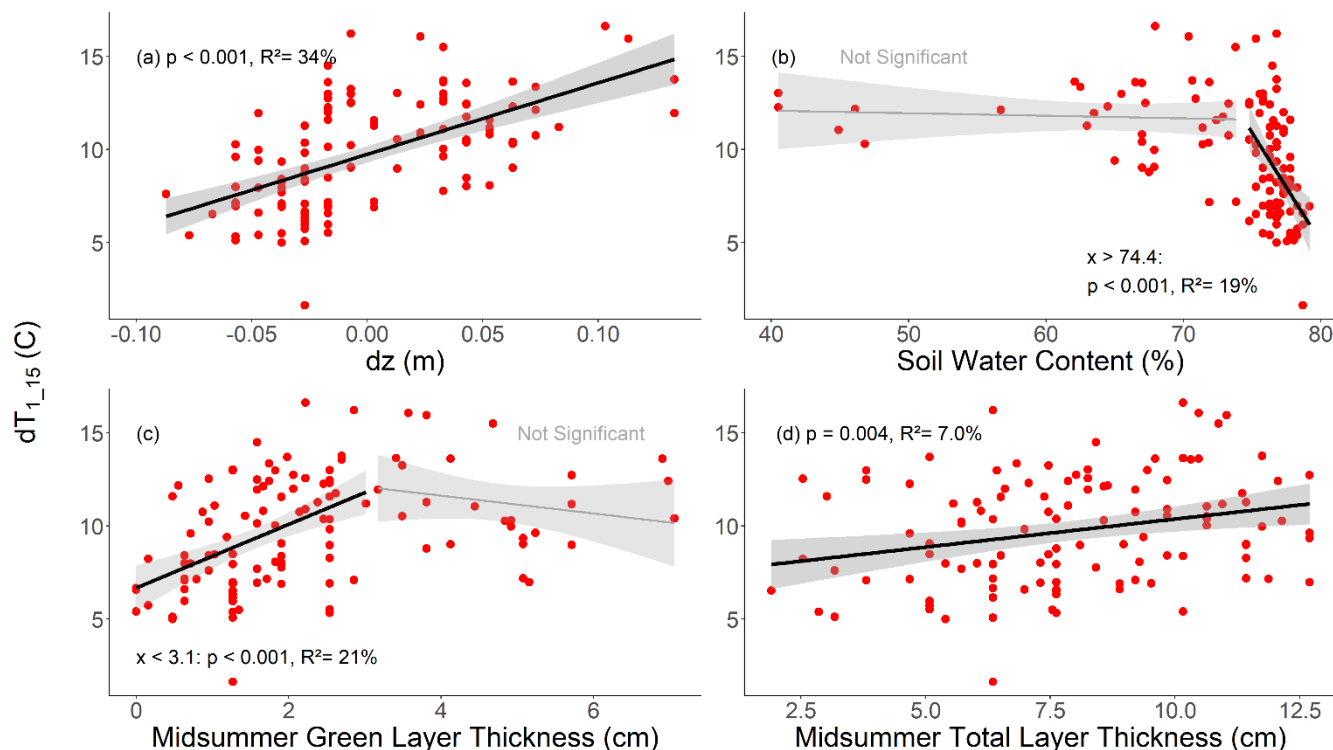


x > 3.1: 4.6% x > 3.1: 0.294 x > 3.1: 125

Total Moss			
Layer Thickness	N/A	Linear: 7.0%	Linear: < 0.001
			Linear: 581

217

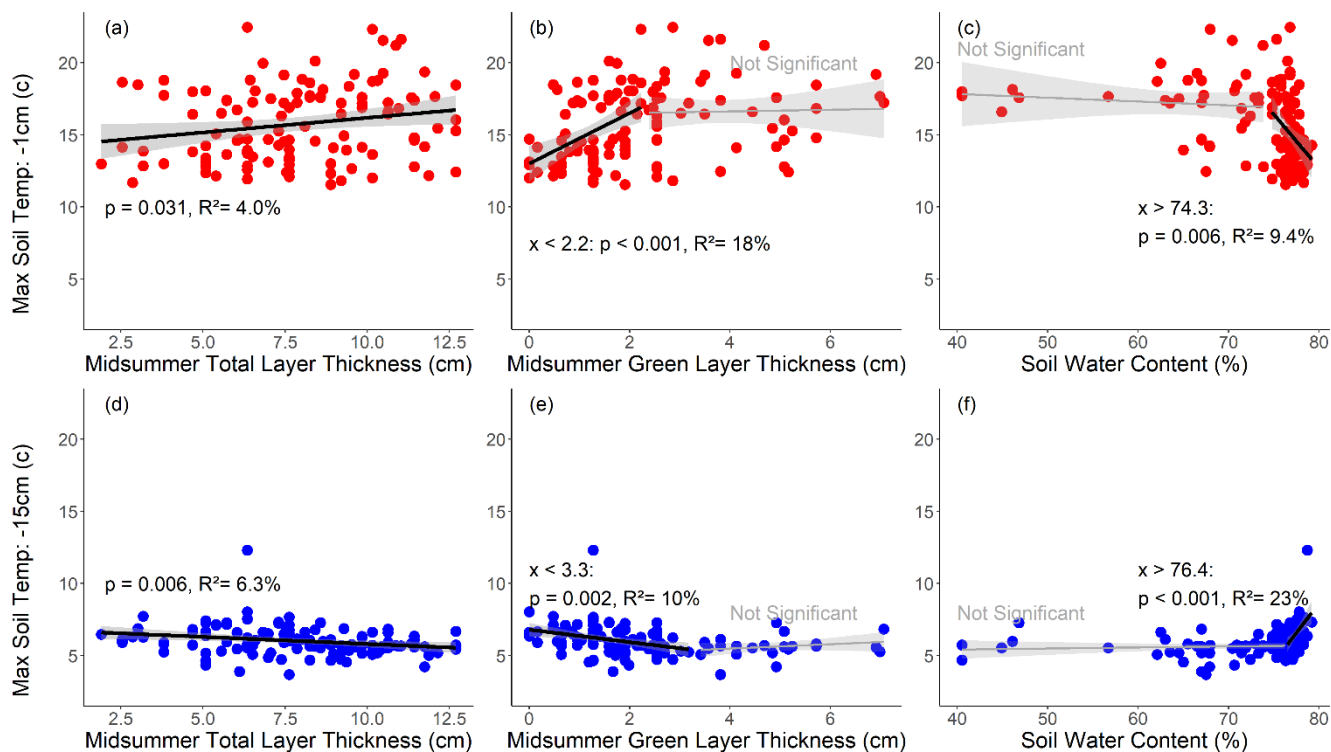
218 We found a negative relationship between the green moss layer thickness and deepest thaw depth (Fig. 2d, p -value = 0.041,
 219 $R^2 = 3.6\%$) and a positive relationship between the green (Fig. 3c, p -value < 0.001, $R^2 = 21\%$ when the green layer thickness
 220 was below 3.1 cm) or total layer thickness (Fig. 3d, p -value < 0.001, $R^2 = 7.0\%$) and dT_{1-15} . A positive relationship was
 221 observed between green (Fig. 4b, p -value < 0.001, $R^2 = 9.7\%$) or total layer thickness (Fig. 4a, p -value = 0.031, $R^2 = 4.0\%$)
 222 and the maximum soil temperature at the surface, but a negative relationship between increasing green (Fig. 4e, p -value =
 223 0.002, $R^2 = 7.9\%$) (or total layer thickness, Fig. 4d, p -value = 0.006, $R^2 = 6.3\%$) and the maximum soil temperature at -15 cm
 224 depths. We observed a negative relationship between the deepest thaw depth and dz (Fig. 2b, p -value < 0.001, $R^2 = 13\%$) and
 225 a positive relationship between dT_{1-15} and dz (Fig. 3a, p -value < 0.001, $R^2 = 34\%$). We noticed a negative relationship between
 226 soil temperatures at -1 cm depths and deepest thaw depth (Fig. 2a, p -value < 0.001, $R^2 = 22\%$). We observed a positive
 227 relationship between increasing green moss layer thickness (Fig. 6b, p -value < 0.001, $R^2 = 13\%$), or total moss layer thickness
 228 (Fig. 6a, p -value < 0.001, $R^2 = 15\%$), and dz.



229

230 **Figure 3: Relationship between the temperature difference (between soil temperature at -1 cm and at -15 cm belowground) and the**
231 **indicated variables for the entire sampling period (summer 2021 and 2022) across all the sampling plots, showing a) a positive**
232 **relationship between the deviation from the mean elevation (dz) and the temperature difference, b) a negative relationship between**
233 **soil water content and the temperature difference when soil water content is greater than 74.4%, c) a positive relationship between**
234 **the green moss layer thickness during the middle of the 2021 summer and the temperature difference when the green moss layer**
235 **thickness was less than 3.1 cm, and d) a positive relationship between the total moss layer thickness and the temperature difference.**

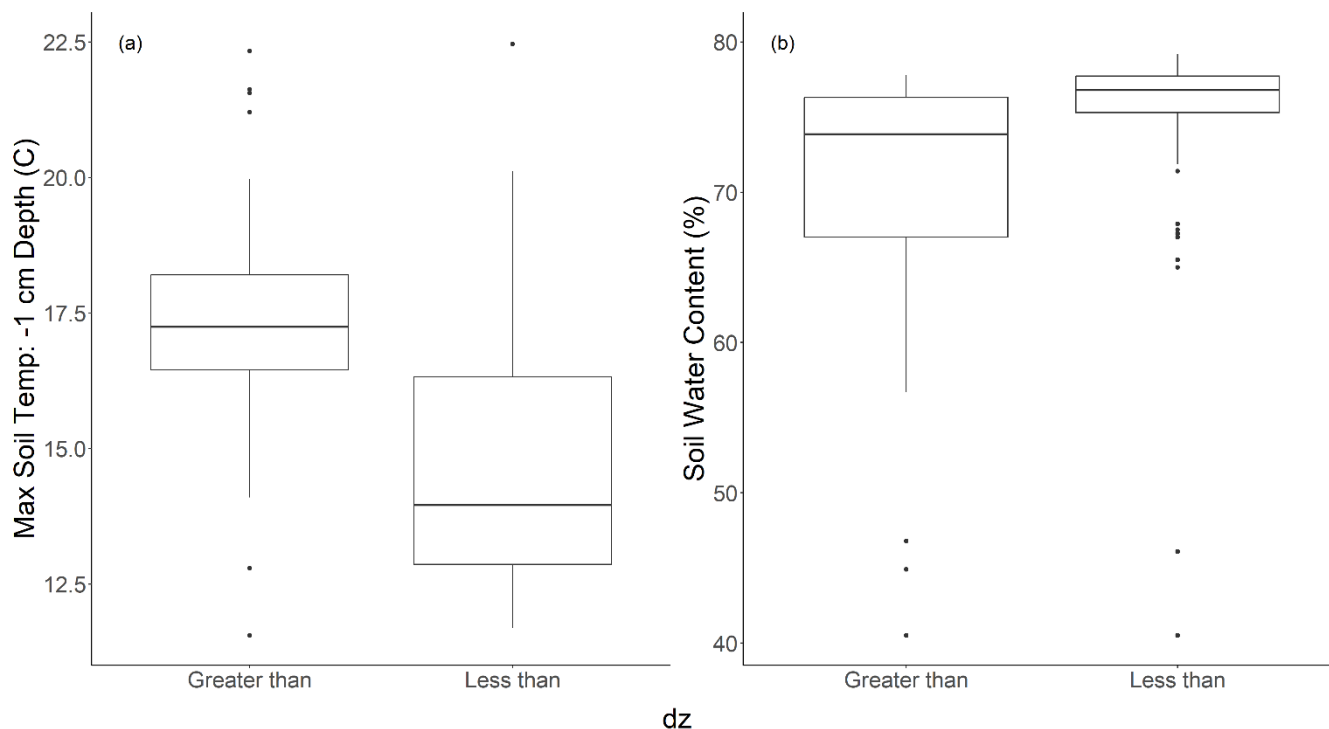
236 Soil water content (soil water content) had a negative relationship with temperature difference when soil water content was
237 greater than 74.4% (Fig. 3b, p -value < 0.001 , $R^2 = 19\%$) and no significant relationship below that threshold. While soil
238 temperatures at -1 cm were negatively associated with soil water content past a threshold of 74.3% (no significant relationship
239 was noted prior to this threshold), the temperature deeper in the soil (15 cm below ground) was positively correlated with soil
240 water content past a soil water content of 76.4% (Fig. 4). A positive relationship was seen between water table level and
241 deepest thaw depth (Fig. 2c, p -value = 0.002, $R^2 = 7.8\%$).



242

243 **Figure 4: Relationships between the maximum soil temperature and the indicated variables for the entire periods of measurements**
244 **aggregated (summer 2021 and 2022), and for all the sampling plots. While green and total moss layer thicknesses was positively**
245 **associated with higher temperatures closer to the surface (a and b), thicker moss layers were associated with cooler temperatures at**
246 **deeper depths (d and e). As the percent soil water content increased, the superficial temperatures decreased (c) but temperature in**
247 **deeper soil layers increased (f).**

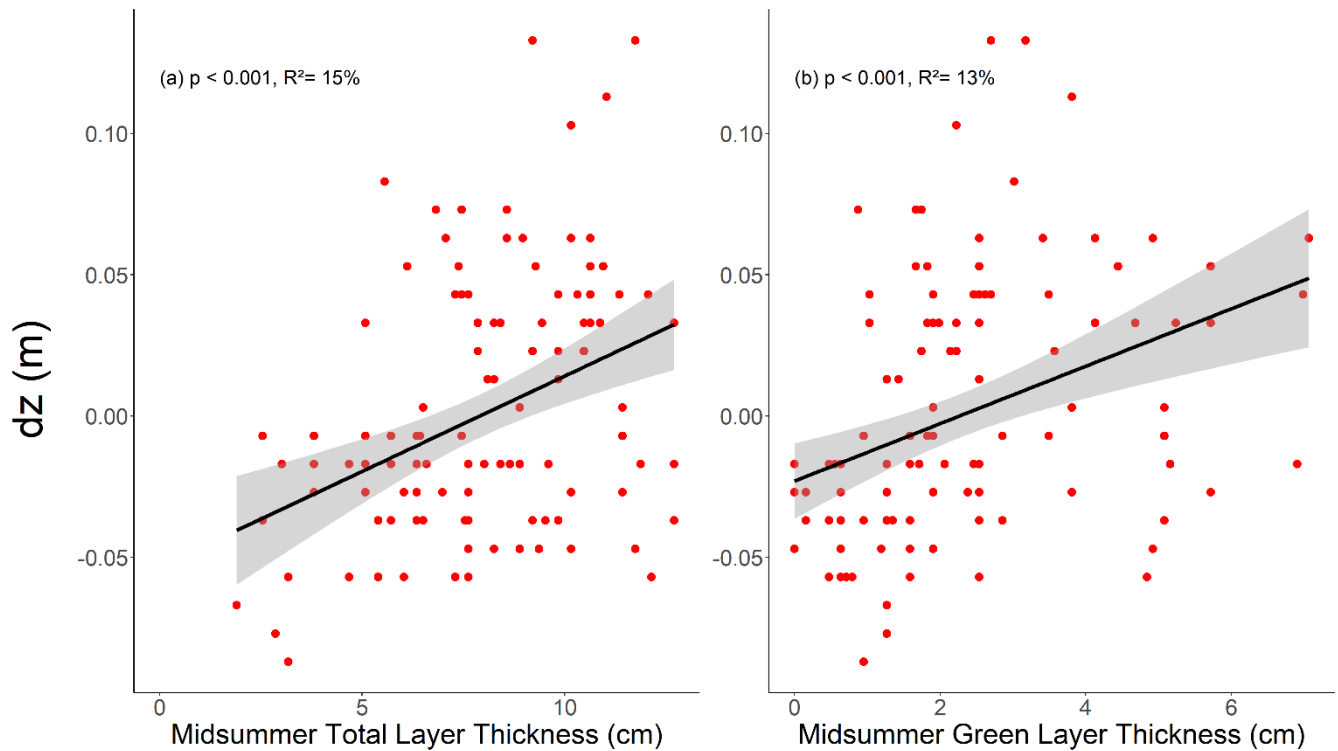
248 Given the significant relationship between soil temperature and relative elevation, we conducted a two-sample t-test to compare
249 surface temperatures at -1 cm depth across both transects in areas above and below the mean elevation. There was a significant
250 difference in temperature between areas above the mean elevation (4.2 cm) and below the mean elevation. The median
251 temperature of higher elevation areas was ($M = 17.3 \pm 4.3$ °C) and those below the mean elevation ($M = 14.8 \pm 4.9$ °C);
252 $t(107.85) = 5.8$, $p < 0.001$, Fig. 5. Another two-sample t-test showed percent soil water content was lower in areas with
253 elevations above the mean elevation ($M = 70.6 \pm 17.4\%$) compared with areas below the mean elevation ($M = 74.7 \pm 12.8\%$)
254 ($p = 0.007$), as shown in Fig. 5, and summarized in Fig. 7.



255

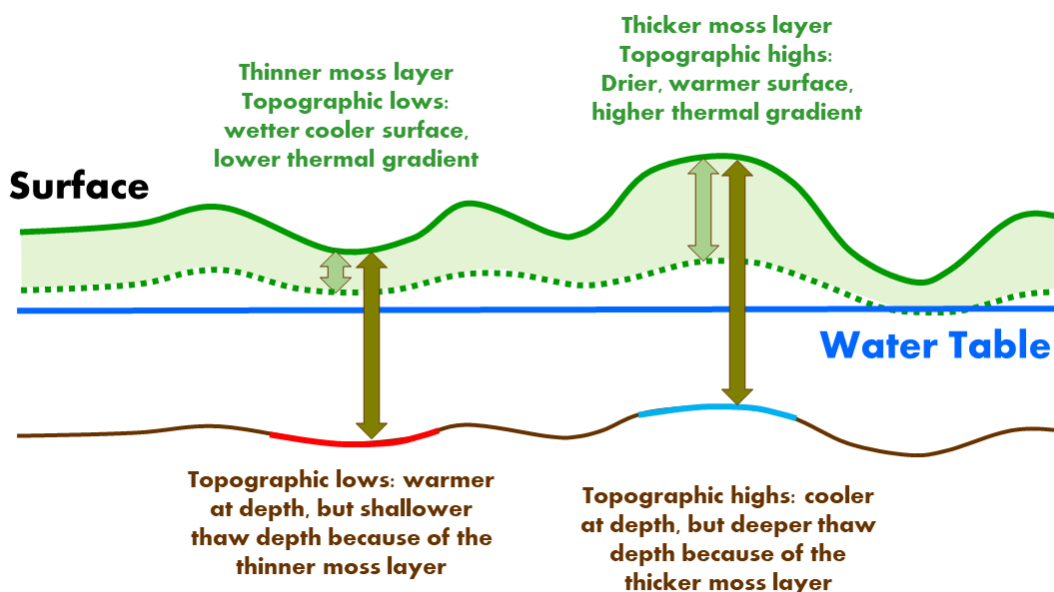
256

257 **Figure 5: Comparison of (a) maximum soil temperature ranges at a -1 cm depth and (b) soil water content based on the deviation**
258 **from the mean elevation (dz) grouped by areas greater than and less than the mean elevation for the entire periods of**
259 **measurements (summer 2021 and 2022), and for all the sampling plots. a) Areas with higher elevations had a higher observed**
260 **average soil temperature. b) Areas with lower observed average soil water content.**



261

262 **Figure 6: Relationships between (a) increasing midsummer (2021) total layer thickness or (b) midsummer (2021) green layer**
263 **thickness and the deviation from the mean elevation (dz) suggesting the occurrence of a thicker moss layer in higher topographic**
264 **areas.**



265

266 **Figure 7: A visual summary of the relationships highlighted by the regression analyses highlighting how thinner moss layers have**
267 **a seemingly shallower depth of thaw and lower surface but higher belowground temperatures as opposed to thicker moss layers**
268 **that have higher surface temperatures and seemingly deeper depth of thaw but lower belowground temperatures.**

269

270 **5 Discussion**

271 We found that moss layer thickness, microtopography, and soil moisture exerted important controls on soil temperature
272 profiles. Microtopographic lower elevation areas had higher soil water content and lower temperature gradients than
273 topographic highs. Thicker green moss layers co-occurred with cooler deep (-15 cm below the surface) soil temperature,
274 which is consistent with a higher thermal insulation (Beringer et al., 2005; Fisher et al., 2016; Hrbáček et al., 2020;
275 Soudzilovskaia et al., 2017). Thicker mosses insulate the soil (Blok et al., 2011; Chadburn et al., 2015; Heijmans et al., 2022;
276 Hrbáček et al., 2020; Park et al., 2018) as shown by the cooler deeper soil temperature, even with warmer near surface (i.e. -
277 1 cm) temperatures. Moss thickness was higher in higher elevation areas possibly because their higher surface temperature



278 might have stimulated moss growth, in these temperature limited ecosystems (Harley et al., 1989; Bengtsson et al., 2021).
279 Near surface temperature was the main control on thaw depth, consistent with previous studies (Dafflon et al., 2017; Schuur
280 et al., 2015). Soil moisture was also a very relevant control on soil temperature, with opposite relationships for the near
281 surface and deeper soil temperatures. Cooler near surface temperature co-occurred with higher soil moisture and could be
282 explained by the higher evaporative cooling of a wetter moss layer (Heijmans et al., 2004a, b) and by the higher thermal
283 conductivity and rates of heat transfer to lower soil layers. The higher thermal conductivity and heat penetration in wetter
284 soils could also explain the higher soil temperature in deeper soil layers (-15 cm) (Soudzilovskaia et al., 2013; Fisher et al.,
285 2016; Hrbáček et al., 2020; Soudzilovskaia et al., 2017; Curasi et al., 2016; Hinkel and Nelson, 2003; Hinkel et al., 2001;
286 Shiklomanov et al., 2010).

287 We observed a significant breakpoint, and different linear regressions for the shallower (~2-3 cm) than deeper green (living)
288 moss layers in describing the relationship between green moss layer thickness and temperatures at -1 cm and -15 cm. This
289 would suggest that the top living layer of mosses has the most relevant role in regulating soil temperature. The larger
290 importance of the top moss layer in insulating the soil is consistent with the reported significant relationship between the top
291 ~15-20 cm of the moss layer moss layer thickness and permafrost thaw (Douglass et al., 2008). The significance in the
292 breakpoint was only observed for the relationship between the green layer thickness and soil temperatures (at -1 cm and at -
293 15 cm depth), while no significant breakpoint was observed in the relationship between the total moss thickness and soil
294 temperatures. This is likely because of the higher water retention of the handlike structures (papillae) present in the green
295 moss layer (Clymo, 1970; Dykas, 2018), which could increase their importance in regulating the heat transfer. Similarly, the
296 lack of a significant response between temperatures at -1 and -15 cm and soil moisture until approximately 74.3% and 76.4%
297 respectively, is consistent with the observed exponential relationship between the thermal conductivity and relative moisture
298 content reported for bryophytes and lichen in permafrost ecosystems, with a steeper relationship at higher moisture levels
299 (Porada et al., 2016). Overall, the relationship between deviation from mean elevation (dz) and moss thickness together with
300 the relationships between moss thickness and -15 cm temperatures confirms that microtopography dominated ecosystem
301 functioning in these arctic tundra ecosystems (Zona et al., 2011; Wilkman et al., 2018).



302

303 **6 Conclusion**

304 The results of this study support the importance of mosses and soil moisture to insulate permafrost. A thicker moss layer is
305 associated with warmer near surface temperature but with cooler deeper soil temperature and larger thermal gradient because
306 of higher thermal insulation. Future studies should better define the role of moisture on heat penetration to deeper soil layers,
307 across a wider range of soil moisture, as this study was mostly focused on very wet ecosystems. Additionally, a wider range
308 of moss thickness together with the role of other vegetation types should be considered when modelling the soil temperature
309 and thaw depth to understand the controls on the integrity of permafrost.

310

311 **7 Data Availability**

312 Donatella Zona, & Kevin Gonzalez. (2023). *Environmental and vegetation control on active layer and soil temperature in an*
313 *Arctic tundra ecosystem in Alaska*. Arctic Data Center. urn:uuid:0e00e7c3-d2a1-4065-bba6-3c664b983990.

314

315 **8 Author Contribution**

316 DZ and WCO acquired funding to support the project leading to this publication. DZ conceptualized the project with KG
317 conducting the investigation process involving data collection. KG conducted formal analysis with contributions from DZ
318 and TB. KG prepared the manuscript with contributions and critical review from all co-authors. All co-authors provided
319 feedback on the data analysis and contributed to writing the manuscript.

320

321 **9 Competing Interests**



322 The authors declare that they have no conflict of interest.

323 **10 Acknowledgements**

324 This study was funded by the Office of Polar Programs of the National Science Foundation (NSF) and awarded to D.Z.,
325 W.C.O. (award numbers 2149988 and 1932900) with additional support by the ABoVE (80NSSC21K1350) Program. The
326 Alaskan sites are on land owned by the Ukpeaġvik Iñupiat Corporation (UIC) and are a part of Iñupiat indigenous
327 community. K.G. and F.T. are supported in part by the NOAA Educational Partnership Program/Minority-Serving
328 Institutions award NA22SEC4810016 Center for Earth System Sciences and Remote Sensing Technologies II. Contents are
329 solely the responsibility of the author(s) and do not represent the official views of NOAA or the U.S. Department of
330 Commerce.



331 References

- 332 Anisimov, O. A., Shiklomanov, N. I., and Nelson, F. E.: Global warming and active-layer thickness: results from transient
333 general circulation models, *Global and Planetary Change*, 15, 61–77, [https://doi.org/10.1016/S0921-8181\(97\)00009-X](https://doi.org/10.1016/S0921-8181(97)00009-X), 1997.
- 334 Arndt, K. A., Lipson, D. A., Hashemi, J., Oechel, W. C., and Zona, D.: Snow melt stimulates ecosystem respiration in Arctic
335 ecosystems, *Global Change Biology*, 26, 5042–5051, <https://doi.org/10.1111/gcb.15193>, 2020.
- 336 Bengtsson, F., Rydin, H., Baltzer, J. L., Bragazza, L., Bu, Z.-J., Caporn, S. J. M., Dorrepaal, E., Flatberg, K. I., Galanina, O.,
337 Gałka, M., Ganeva, A., Goia, I., Goncharova, N., Hájek, M., Haraguchi, A., Harris, L. I., Humphreys, E., Jiroušek, M.,
338 Kajukalo, K., Karofeld, E., Koronatova, N. G., Kosykh, N. P., Laine, A. M., Lamentowicz, M., Lapshina, E., Limpens, J.,
339 Linkosalmi, M., Ma, J.-Z., Mauritz, M., Mitchell, E. A. D., Munir, T. M., Natali, S. M., Natcheva, R., Payne, R. J., Philippov,
340 D. A., Rice, S. K., Robinson, S., Robroek, B. J. M., Rochefort, L., Singer, D., Stenøien, H. K., Tuittila, E.-S., Vellak, K.,
341 Waddington, J. M., and Granath, G.: Environmental drivers of Sphagnum growth in peatlands across the Holarctic region,
342 *Journal of Ecology*, 109, 417–431, <https://doi.org/10.1111/1365-2745.13499>, 2021.
- 343 Beringer, J., Chapin, F. S., Thompson, C. C., and McGuire, A. D.: Surface energy exchanges along a tundra-forest transition
344 and feedbacks to climate, *Agricultural and Forest Meteorology*, 131, 143–161,
345 <https://doi.org/10.1016/j.agrformet.2005.05.006>, 2005.
- 346 Blok, D., Heijmans, M. M. P. D., Schaepman-Strub, G., Kononov, A. V., Maximov, T. C., and Berendse, F.: Shrub expansion
347 may reduce summer permafrost thaw in Siberian tundra, *Global Change Biology*, 16, 1296–1305,
348 <https://doi.org/10.1111/j.1365-2486.2009.02110.x>, 2010.
- 349 Blok, D., Heijmans, M. M. P. D., Schaepman-Strub, G., van Ruijven, J., Parmentier, F. J. W., Maximov, T. C., and Berendse,
350 F.: The Cooling Capacity of Mosses: Controls on Water and Energy Fluxes in a Siberian Tundra Site, *Ecosystems*, 14, 1055–
351 1065, <https://doi.org/10.1007/s10021-011-9463-5>, 2011.



- 352 Boisvert, L. N. and Stroeve, J. C.: The Arctic is becoming warmer and wetter as revealed by the Atmospheric Infrared Sounder,
353 Geophysical Research Letters, 42, 4439–4446, <https://doi.org/10.1002/2015GL063775>, 2015.
- 354 Chadburn, S., Burke, E., Essery, R., Boike, J., Langer, M., Heikenfeld, M., Cox, P., and Friedlingstein, P.: An improved
355 representation of physical permafrost dynamics in the JULES land-surface model, Geoscientific Model Development, 8, 1493–
356 1508, <https://doi.org/10.5194/gmd-8-1493-2015>, 2015.
- 357 Clymo, R. S.: The Growth of Sphagnum: Methods of Measurement, Journal of Ecology, 58, 13–49,
358 <https://doi.org/10.2307/2258168>, 1970.
- 359 Curasi, S. R., Loranty, M. M., and Natali, S. M.: Water track distribution and effects on carbon dioxide flux in an eastern
360 Siberian upland tundra landscape, Environ. Res. Lett., 11, 045002, <https://doi.org/10.1088/1748-9326/11/4/045002>, 2016.
- 361 Dafflon, B., Oktem, R., Peterson, J., Ulrich, C., Tran, A. P., Romanovsky, V., and Hubbard, S. S.: Coincident aboveground
362 and belowground autonomous monitoring to quantify covariability in permafrost, soil, and vegetation properties in Arctic
363 tundra, Journal of Geophysical Research: Biogeosciences, 122, 1321–1342, <https://doi.org/10.1002/2016JG003724>, 2017.
- 364 Dai, A., Luo, D., Song, M., and Liu, J.: Arctic amplification is caused by sea-ice loss under increasing CO₂, Nat Commun, 10,
365 121, <https://doi.org/10.1038/s41467-018-07954-9>, 2019.
- 366 Davidson, E. A. and Janssens, I. A.: Temperature sensitivity of soil carbon decomposition and feedbacks to climate change,
367 Nature, 440, 165–173, <https://doi.org/10.1038/nature04514>, 2006.
- 368 Davidson, S. J., Sloan, V. L., Phoenix, G. K., Wagner, R., Fisher, J. P., Oechel, W. C., and Zona, D.: Vegetation Type
369 Dominates the Spatial Variability in CH₄ Emissions Across Multiple Arctic Tundra Landscapes, Ecosystems, 19, 1116–1132,
370 <https://doi.org/10.1007/s10021-016-9991-0>, 2016.
- 371 Douglas, T. A., Kanevskiy, M. Z., Romanovsky, V. E., Shur, Y., and Yoshikawa, K.: Permafrost Dynamics at the Fairbanks
372 Permafrost Experimental Station Near Fairbanks, Alaska, n.d.



- 373 Dykas, C.: Water Holding Capacity in Sphagnum: Micro CT Scanning Reveals Differences in Pore Structure, Honors Theses,
374 2018.
- 375 Euskirchen, E. S., McGuire, A. D., Chapin III, F. S., Yi, S., and Thompson, C. C.: Changes in vegetation in northern Alaska
376 under scenarios of climate change, 2003–2100: implications for climate feedbacks, *Ecological Applications*, 19, 1022–1043,
377 <https://doi.org/10.1890/08-0806.1>, 2009.
- 378 Fisher, J. B., Hayes, D. J., Schwalm, C. R., Huntzinger, D. N., Stofferahn, E., Schaefer, K., Luo, Y., Wullschleger, S. D.,
379 Goetz, S., Miller, C. E., Griffith, P., Chadburn, S., Chatterjee, A., Ciais, P., Douglas, T. A., Genet, H., Ito, A., Neigh, C. S. R.,
380 Poulter, B., Rogers, B. M., Sonnentag, O., Tian, H., Wang, W., Xue, Y., Yang, Z.-L., Zeng, N., and Zhang, Z.: Missing pieces
381 to modeling the Arctic-Boreal puzzle, *Environ. Res. Lett.*, 13, 020202, <https://doi.org/10.1088/1748-9326/aa9d9a>, 2018.
- 382 Fisher, J. P., Estop-Aragónés, C., Thierry, A., Charman, D. J., Wolfe, S. A., Hartley, I. P., Murton, J. B., Williams, M., and
383 Phoenix, G. K.: The influence of vegetation and soil characteristics on active-layer thickness of permafrost soils in boreal
384 forest, *Global Change Biology*, 22, 3127–3140, <https://doi.org/10.1111/gcb.13248>, 2016.
- 385 Fujinami, H., Yasunari, T., and Watanabe, T.: Trend and interannual variation in summer precipitation in eastern Siberia in
386 recent decades, *International Journal of Climatology*, 36, 355–368, <https://doi.org/10.1002/joc.4352>, 2016.
- 387 Gornall, J. L., Jónsdóttir, I. S., Woodin, S. J., and Van der Wal, R.: Arctic mosses govern below-ground environment and
388 ecosystem processes, *Oecologia*, 153, 931–941, <https://doi.org/10.1007/s00442-007-0785-0>, 2007.
- 389 Harley, P. C., Tenhunen, J. D., Murray, K. J., and Beyers, J.: Irradiance and temperature effects on photosynthesis of tussock
390 tundra Sphagnum mosses from the foothills of the Philip Smith Mountains, Alaska, *Oecologia*, 79, 251–259,
391 <https://doi.org/10.1007/BF00388485>, 1989.
- 392 Hayashi, M., Goeller, N., Quinton, W. L., and Wright, N.: A simple heat-conduction method for simulating the frost-table
393 depth in hydrological models, *Hydrological Processes*, 21, 2610–2622, <https://doi.org/10.1002/hyp.6792>, 2007.



- 394 Heijmans, M. M. P. D., Arp, W. J., and Chapin, F. S.: Carbon dioxide and water vapour exchange from understory species in
395 boreal forest, *Agricultural and Forest Meteorology*, 123, 135–147, <https://doi.org/10.1016/j.agrformet.2003.12.006>, 2004a.
- 396 Heijmans, M. M. P. D., Arp, W. J., and Chapin III, F. S.: Controls on moss evaporation in a boreal black spruce forest, *Global*
397 *Biogeochemical Cycles*, 18, <https://doi.org/10.1029/2003GB002128>, 2004b.
- 398 Heijmans, M. M. P. D., Magnússon, R. Í., Lara, M. J., Frost, G. V., Myers-Smith, I. H., van Huissteden, J., Jorgenson, M. T.,
399 Fedorov, A. N., Epstein, H. E., Lawrence, D. M., and Limpens, J.: Tundra vegetation change and impacts on permafrost, *Nat*
400 *Rev Earth Environ*, 3, 68–84, <https://doi.org/10.1038/s43017-021-00233-0>, 2022.
- 401 Hinkel, K. M. and Nelson, F. E.: Spatial and temporal patterns of active layer thickness at Circumpolar Active Layer
402 Monitoring (CALM) sites in northern Alaska, 1995–2000, *Journal of Geophysical Research: Atmospheres*, 108,
403 <https://doi.org/10.1029/2001JD000927>, 2003.
- 404 Hinkel, K. M., Paetzold, F., Nelson, F. E., and Bockheim, J. G.: Patterns of soil temperature and moisture in the active layer
405 and upper permafrost at Barrow, Alaska: 1993–1999, *Global and Planetary Change*, 29, 293–309,
406 [https://doi.org/10.1016/S0921-8181\(01\)00096-0](https://doi.org/10.1016/S0921-8181(01)00096-0), 2001.
- 407 Hrbáček, F., Cannone, N., Kňazková, M., Malfasi, F., Convey, P., and Guglielmin, M.: Effect of climate and moss vegetation
408 on ground surface temperature and the active layer among different biogeographical regions in Antarctica, *CATENA*, 190,
409 104562, <https://doi.org/10.1016/j.catena.2020.104562>, 2020.
- 410 Hugelius, G., Strauss, J., Zubrzycki, S., Harden, J. W., Schuur, E. a. G., Ping, C.-L., Schirrmeister, L., Grosse, G., Michaelson,
411 G. J., Koven, C. D., O'Donnell, J. A., Elberling, B., Mishra, U., Camill, P., Yu, Z., Palmtag, J., and Kuhry, P.: Estimated stocks
412 of circumpolar permafrost carbon with quantified uncertainty ranges and identified data gaps, *Biogeosciences*, 11, 6573–6593,
413 <https://doi.org/10.5194/bg-11-6573-2014>, 2014.
- 414 van Huissteden, J. and Dolman, A.: Soil carbon in the Arctic and the permafrost carbon feedback, *Current Opinion in*
415 *Environmental Sustainability*, 4, 545–551, <https://doi.org/10.1016/j.cosust.2012.09.008>, 2012.



- 416 Koven, C. D., Ringeval, B., Friedlingstein, P., Ciais, P., Cadule, P., Khvorostyanov, D., Krinner, G., and Tarnocai, C.:
417 Permafrost carbon-climate feedbacks accelerate global warming, *Proceedings of the National Academy of Sciences*, 108,
418 14769–14774, <https://doi.org/10.1073/pnas.1103910108>, 2011.
- 419 Kuhn, M.: caret: Classification and Regression Training, *Astrophysics Source Code Library*, ascl:1505.003, 2015.
- 420 Lumley, T., and A. Miller. 2022. leaps: Regression Subset Selection. R package version 3.1, [https://CRAN.R-](https://CRAN.R-project.org/package=leaps)
421 [project.org/package=leaps](https://CRAN.R-project.org/package=leaps).
- 422 Luo, Y., Ahlström, A., Allison, S. D., Batjes, N. H., Brovkin, V., Carvalhais, N., Chappell, A., Ciais, P., Davidson, E. A.,
423 Finzi, A., Georgiou, K., Guenet, B., Hararuk, O., Harden, J. W., He, Y., Hopkins, F., Jiang, L., Koven, C., Jackson, R. B.,
424 Jones, C. D., Lara, M. J., Liang, J., McGuire, A. D., Parton, W., Peng, C., Randerson, J. T., Salazar, A., Sierra, C. A., Smith,
425 M. J., Tian, H., Todd-Brown, K. E. O., Torn, M., van Groenigen, K. J., Wang, Y. P., West, T. O., Wei, Y., Wieder, W. R.,
426 Xia, J., Xu, X., Xu, X., and Zhou, T.: Toward more realistic projections of soil carbon dynamics by Earth system models,
427 *Global Biogeochemical Cycles*, 30, 40–56, <https://doi.org/10.1002/2015GB005239>, 2016.
- 428 Miner, K. R., D’Andrilli, J., Mackelprang, R., Edwards, A., Malaska, M. J., Waldrop, M. P., and Miller, C. E.: Emergent
429 biogeochemical risks from Arctic permafrost degradation, *Nat. Clim. Chang.*, 11, 809–819, [https://doi.org/10.1038/s41558-](https://doi.org/10.1038/s41558-021-01162-y)
430 [021-01162-y](https://doi.org/10.1038/s41558-021-01162-y), 2021.
- 431 Miner, K. R., Turetsky, M. R., Malina, E., Bartsch, A., Tamminen, J., McGuire, A. D., Fix, A., Sweeney, C., Elder, C. D., and
432 Miller, C. E.: Permafrost carbon emissions in a changing Arctic, *Nat Rev Earth Environ*, 3, 55–67,
433 <https://doi.org/10.1038/s43017-021-00230-3>, 2022.
- 434 Muggeo, V. M. R.: Estimating regression models with unknown break-points, *Statistics in Medicine*, 22, 3055–3071,
435 <https://doi.org/10.1002/sim.1545>, 2003.
- 436 Muggeo, V.M.R. (2008) Segmented: an R package to fit regression models with broken-line relationships. *R News* 8/1, 20–
437 25.



- 438 Nicolsky, D. J., Romanovsky, V. E., and Panteleev, G. G.: Estimation of soil thermal properties using in-situ temperature
439 measurements in the active layer and permafrost, *Cold Regions Science and Technology*, 55, 120–129,
440 <https://doi.org/10.1016/j.coldregions.2008.03.003>, 2009.
- 441 Park, H., Launiainen, S., Konstantinov, P. Y., Iijima, Y., and Fedorov, A. N.: Modeling the Effect of Moss Cover on Soil
442 Temperature and Carbon Fluxes at a Tundra Site in Northeastern Siberia, *Journal of Geophysical Research: Biogeosciences*,
443 123, 3028–3044, <https://doi.org/10.1029/2018JG004491>, 2018.
- 444 Permafrost Subcommittee: 1988, Glossary of permafrost and related ground-ice terms, Associate Committee on Geotechnical
445 Research, National Research Council of Canada, Ottawa, Technical Memorandum No. 142, 156 pp., 1988.
- 446 Porada, P., Ekici, A., and Beer, C.: Effects of bryophyte and lichen cover on permafrost soil temperature at large scale, *The*
447 *Cryosphere*, 10, 2291–2315, <https://doi.org/10.5194/tc-10-2291-2016>, 2016.
- 448 Posit Team. 2022. RStudio: Integrated Development Environment for R. Posit Software, PBC, Boston, MA.
449 <http://www.posit.co/>.
- 450 R Core Team. 2022. R: A language and environment for statistical computing. R Foundation for Statistical Computing, Vienna,
451 Austria. <https://www.R-project.org/>.
- 452 Schaefer, K., Lantuit, H., Romanovsky, V. E., Schuur, E. A. G., and Witt, R.: The impact of the permafrost carbon feedback
453 on global climate, *Environ. Res. Lett.*, 9, 085003, <https://doi.org/10.1088/1748-9326/9/8/085003>, 2014.
- 454 Schaphoff, S., Heyder, U., Ostberg, S., Gerten, D., Heinke, J., and Lucht, W.: Contribution of permafrost soils to the global
455 carbon budget, *Environ. Res. Lett.*, 8, 014026, <https://doi.org/10.1088/1748-9326/8/1/014026>, 2013.
- 456 Schuur, E. A. G., Bockheim, J., Canadell, J. G., Euskirchen, E., Field, C. B., Goryachkin, S. V., Hagemann, S., Kuhry, P.,
457 Lafleur, P. M., Lee, H., Mazhitova, G., Nelson, F. E., Rinke, A., Romanovsky, V. E., Shiklomanov, N., Tarnocai, C., Venevsky,



- 458 S., Vogel, J. G., and Zimov, S. A.: Vulnerability of Permafrost Carbon to Climate Change: Implications for the Global Carbon
459 Cycle, *BioScience*, 58, 701–714, <https://doi.org/10.1641/B580807>, 2008.
- 460 Schuur, E. A. G., McGuire, A. D., Schädel, C., Grosse, G., Harden, J. W., Hayes, D. J., Hugelius, G., Koven, C. D., Kuhry,
461 P., Lawrence, D. M., Natali, S. M., Olefeldt, D., Romanovsky, V. E., Schaefer, K., Turetsky, M. R., Treat, C. C., and Vonk, J.
462 E.: Climate change and the permafrost carbon feedback, *Nature*, 520, 171–179, <https://doi.org/10.1038/nature14338>, 2015.
- 463 Schuur, T.: Permafrost and the Global Carbon Cycle, 2019. [https://arctic.noaa.gov/Report-Card/Report-Card-](https://arctic.noaa.gov/Report-Card/Report-Card-2019/ArtMID/7916/ArticleID/844/Permafrost-and-the-Global-Carbon-Cycle)
464 [2019/ArtMID/7916/ArticleID/844/Permafrost-and-the-Global-Carbon-Cycle](https://arctic.noaa.gov/Report-Card/Report-Card-2019/ArtMID/7916/ArticleID/844/Permafrost-and-the-Global-Carbon-Cycle).
- 465 Shiklomanov, N. I., Streletskiy, D. A., Nelson, F. E., Hollister, R. D., Romanovsky, V. E., Tweedie, C. E., Bockheim, J. G.,
466 and Brown, J.: Decadal variations of active-layer thickness in moisture-controlled landscapes, Barrow, Alaska, *Journal of*
467 *Geophysical Research: Biogeosciences*, 115, <https://doi.org/10.1029/2009JG001248>, 2010.
- 468 Soudzilovskaia, N. A., van Bodegom, P. M., and Cornelissen, J. H. C.: Dominant bryophyte control over high-latitude soil
469 temperature fluctuations predicted by heat transfer traits, field moisture regime and laws of thermal insulation, *Functional*
470 *Ecology*, 27, 1442–1454, <https://doi.org/10.1111/1365-2435.12127>, 2013.
- 471 Turunen, M., Hyväluoma, J., Heikkinen, J., Keskinen, R., Kaseva, J., Hannula, M., and Rasa, K.: Quantifying the pore structure
472 of different biochars and their impacts on the water retention properties of Sphagnum moss growing media, *Biosystems*
473 *Engineering*, 191, 96–106, <https://doi.org/10.1016/j.biosystemseng.2020.01.006>, 2020.
- 474 Venables, W. N., and B.D. Ripley (2002) *Modern Applied Statistics with S*. Fourth Edition. Springer, New York. ISBN 0-
475 387-95457-0
- 476 van der Wal, R., van Lieshout, S. M. J., and Loonen, M. J. J. E.: Herbivore impact on moss depth, soil temperature and arctic
477 plant growth, *Polar Biol*, 24, 29–32, <https://doi.org/10.1007/s003000000170>, 2001.



- 478 Wilkman, E., Zona, D., Tang, Y., Gioli, B., Lipson, D. A., and Oechel, W.: Temperature Response of Respiration Across the
479 Heterogeneous Landscape of the Alaskan Arctic Tundra, *Journal of Geophysical Research: Biogeosciences*, 123, 2287–2302,
480 <https://doi.org/10.1029/2017JG004227>, 2018.
- 481 Williams, M., Zhang, Y., Estop-Aragonés, C., Fisher, J. P., Xenakis, G., Charman, D. J., Hartley, I. P., Murton, J. B., and
482 Phoenix, G. K.: Boreal permafrost thaw amplified by fire disturbance and precipitation increases, *Environ. Res. Lett.*, 15,
483 114050, <https://doi.org/10.1088/1748-9326/abbeb8>, 2020.
- 484 Zona, D., Oechel, W. C., Kochendorfer, J., Paw U, K. T., Salyuk, A. N., Olivas, P. C., Oberbauer, S. F., and Lipson, D. A.:
485 Methane fluxes during the initiation of a large-scale water table manipulation experiment in the Alaskan Arctic tundra, *Global*
486 *Biogeochemical Cycles*, 23, <https://doi.org/10.1029/2009GB003487>, 2009.
- 487 Zona, D., Lipson, D. A., Zulueta, R. C., Oberbauer, S. F., and Oechel, W. C.: Microtopographic controls on ecosystem
488 functioning in the Arctic Coastal Plain, *Journal of Geophysical Research: Biogeosciences*, 116,
489 <https://doi.org/10.1029/2009JG001241>, 2011.
- 490 Zona, D., Lipson, D. A., Paw U, K. T., Oberbauer, S. F., Olivas, P., Gioli, B., and Oechel, W. C.: Increased CO₂ loss from
491 vegetated drained lake tundra ecosystems due to flooding, *Global Biogeochemical Cycles*, 26,
492 <https://doi.org/10.1029/2011GB004037>, 2012.
- 493 Zona, D., Gioli, B., Commane, R., Lindaas, J., Wofsy, S. C., Miller, C. E., Dinardo, S. J., Dengel, S., Sweeney, C., Karion,
494 A., Chang, R. Y.-W., Henderson, J. M., Murphy, P. C., Goodrich, J. P., Moreaux, V., Liljedahl, A., Watts, J. D., Kimball, J.
495 S., Lipson, D. A., and Oechel, W. C.: Cold season emissions dominate the Arctic tundra methane budget, *Proceedings of the*
496 *National Academy of Sciences*, 113, 40–45, <https://doi.org/10.1073/pnas.1516017113>, 2016.
- 497 Zona, D., Lafleur, P. M., Hufkens, K., Gioli, B., Bailey, B., Burba, G., Euskirchen, E. S., Watts, J. D., Arndt, K. A., Farina,
498 M., Kimball, J. S., Heimann, M., Göckede, M., Pallandt, M., Christensen, T. R., Mastepanov, M., López-Blanco, E., Dolman,
499 A. J., Commane, R., Miller, C. E., Hashemi, J., Kutzbach, L., Holl, D., Boike, J., Wille, C., Sachs, T., Kalhori, A., Humphreys,



- 500 E. R., Sonnentag, O., Meyer, G., Gosselin, G. H., Marsh, P., and Oechel, W. C.: Pan-Arctic soil moisture control on tundra
501 carbon sequestration and plant productivity, *Global Change Biology*, 29, 1267–1281, <https://doi.org/10.1111/gcb.16487>, 2023.